Desalination and Water Treatment
www.deswater.com
doi: 10.1080/19443994.2013.780817

51 (2013) 6299–6309
September

Taylor & Francis
Taylor & Francis Group

Experimental comparison of direct contact membrane distillation (DCMD) with vacuum membrane distillation (VMD)

Jaewuk Koo[a], Jihee Han[a], Jinsik Sohn[a], Sangho Lee[a,*], Tae-Mun Hwang[b]

[a]*School of Civil and Environmental Engineering, Kookmin University, Jeongneung-Dong, Seongbuk-Gu, Seoul 136-702, Republic of Korea*
Tel. +82 2 910 4529; Fax: +82 2 910 4939; email: sanghlee@kookmin.ac.kr
[b]*Deparment of Construction Environmental Research Korea Institute of Construction Technology, 2311 Daehwa-Dong, Ilasan-gu, Kyonggi-do, Republic of Korea*

Received 23 October 2012; Accepted 23 December 2012

ABSTRACT

Membrane distillation (MD) is a thermally driven membrane process using porous hydrophobic membranes. MD has been investigated as an alternative desalination technology due to its advantages over multi-stage flash (MSF) and reverse osmosis (RO). Nevertheless, it is difficult to design and optimize the MD systems under various conditions, because both thermal and hydrodynamic effects play an important role. Therefore, this study focused on performance analysis of MD systems in different configurations. Direct contact MD (DCMD) and vacuum MD (VMD) were experimentally compared using laboratory-scale systems. A simple model was also applied to analyze the difference between two configurations theoretically. Experimental results indicated that permeate flux in DCMD and VMD were sensitive to the operating conditions. Using same membranes, two MD systems showed different flux behaviors. The influences of operating parameters for DCMD and VMD on overall efficiency were also investigated. The model results also confirmed the difference between these two systems theoretically.

Keywords: Membrane distillation; Direct contact membrane distillation; Vacuum membrane distillation; Desalination; Water treatment

1. Introduction

Currently, multi-stage flash distillation (MSF) and reverse osmosis (RO) are the most frequently used techniques for desalination of brackish water and seawater [1–5,9]. Nevertheless, new technologies such as membrane distillation (MD) have been widely investigated as cost-efficient alternatives to the existing desalination technologies [1–4]. MD is a thermally driven separation process, in which only vapor molecules are able to pass through a porous hydrophobic membrane. MD is driven by the vapor pressure difference between the porous hydrophobic membrane surfaces. It allows the operation under relatively low temperature conditions ranging from 50 to 80°C [9,10]. These operating temperatures for MD are significantly lower than those of conventional distillation processes

*Corresponding author.

Presented at The Fifth Desalination Workshop (IDW 2012), October 28–31, 2012, Jeju, Korea

such as MSF, which corresponds from 90 to 120˚C [11]. MD also has other attractive features, including high rejection of most inorganic ions (over 99.9%); and capability of high recovery ratio (over 50%).

Nevertheless, it is difficult to design and operate MD systems, because both thermal and hydrodynamic effects play an important role [1–3]. Moreover, the performance of MD systems depends on their configurations. Generally, MD can be divided into the following configurations, based on the different methods to create a vapor pressure difference across the membrane [1,2]: (a) direct contact membrane distillation (DCMD); (b) air gap membrane distillation (AGMD); (c) sweeping gas membrane distillation (SGMD); and (d) vacuum membrane distillation (VMD). In DCMD, the cooling solution is in direct contact with the permeating side of the membrane. In AGMD, the permeated water vapor, after crossing the air gap in the module, is condensed over a cool surface inside the module. A sweeping gas is driving the water vapor out of the system that also condensate out of the system in SGMD, while vacuum carries the water vapor out of the system and condensation occurs outside the module by cooling in VMD.

Among four different configurations, DCMD is the simplest one, which allows relatively high flux and ease of operation. Accordingly, most studies on MD have been done using DCMD systems [9]. Nevertheless, the thermal efficiency (defined as the fraction of heat energy which is only used for evaporation) in DCMD is relatively small. In contrast to DCMD, AGMD has high thermal efficiency but low flux. SGMD has characteristics similar to both DCMD and AGMD, but requires large sweeping gas flows to get significant permeate yield. On the other hand, VMD can achieve high flux and high thermal efficiency, which has potential for successful application to seawater desalination. However, VMD is the least studied configuration [9] due to the inconvenience to set up vacuum equipment and external condensers.

The mechanism of transport in MD involves simultaneous heat and mass transfer from the feed side, across the boundary layer, and membrane, to the permeate side. Accordingly, there are a lot of factors affecting the performance of MD. The hydrophobicity, pore size, and thermal conductivity of membranes are important in determining the MD configurations [6,7]. Operating parameters such as flow rate, temperature difference, and vapor pressure difference are also important [8]. Unlike pressure-driven membrane processes, not only concentration polarization (CP) but also temperature polarization (TP) should be considered in MD. Membrane fouling and pore wetting are key issues to successful application of MD.

In this study, we aimed at the analysis of MD systems under various conditions. Direct contact MD (DCMD) and vacuum MD (VMD) configurations were selected for establishing a comparison of the membrane performances used in these two methods [4]. Both VMD and DCMD systems were developed in laboratory scale and operated under similar conditions. The experimental results were also analyzed using a simple theoretical approach. Based on these results, the potential of VMD and DCMD for seawater desalination were discussed as well.

2. Theoretical analysis

Mathematical models for DCMD and VMD were developed in this study for better understanding of various MD systems. We only give a broad outline of the model here, since details are provided separately. Different mass transfer mechanisms inside the membrane were considered in the model, including molecular diffusion, the Knudsen diffusion, and viscous flow. Concentration polarization and TP were estimated using the Sherwood and Nusselt correlations, respectively. The models were implemented using MATLAB graphical user interface and allow the user to interactively assign parameters values. Table 1 summarizes the model equations used in this study.

3. Experimental method

3.1. Membranes

Commercially-available hydrophobic PVDF (polyvinylidene fluoride) membrane (Millipore, USA) and PTFE (polytetrafluoroethylene) membrane (Millipore, USA) were used. Table 2 summarizes the basic properties of these membranes.

3.2. MD systems

Two laboratory-scale systems for DCMD and VMD were developed for the experimental study. Figs. 1 and 2 illustrate the concepts and schematic diagrams of the experimental setup for these two systems, respectively. Each has membrane modules with same membrane area. In DCMD configuration (Fig. 2(a)), the hot solution (feed) was supplied to directly contact with the hot membrane side surface using a gear pump. The vapor was moved by the pressure difference across the membrane to the permeate side and condensed inside the membrane module. An electronic balance connected to a data logger was used to continuously measure water flux through the

Table 1
Summary of model equations for DCMD and VMD [1,2]

Meaning	Equation	No.
Antoine equation for vapor pressure estimation	$p_w^0(T) = \exp\left(\alpha - \frac{\beta}{\gamma+T}\right)$	(1)
Effect of salt concentration on vapor pressure	$p_w(T, C_s) = \frac{p_w^0(T)}{1+0.57357\frac{C_s}{1-C_s}}$	(2)
Flux equation	$J_i = \frac{B_i}{\rho}(p_w(T_{m,f}, C_{m,f}) - p_w(T_{m,p}, C_{m,p}))$	(3)
Transport coefficient for Knudson diffusion	$B_1 = 1.064\frac{r\varepsilon}{\tau\delta}\left(\frac{M}{RT_m}\right)^{0.5}$	(4)
Transport coefficient for molecular diffusion	$B_2 = \frac{1}{Y_{\ln}}\frac{D\varepsilon}{\tau\delta}\left(\frac{M}{RT_m}\right)^{0.5}$	(5)
Transport coefficient for Poiseuille flow	$B_3 = 0.125\frac{r^2\varepsilon}{\tau\delta}\left(\frac{MP_m}{\mu RT_m}\right)$	(6)
Overall transport coefficient	$B_i = \frac{1}{\left(\frac{1}{B_1}+\frac{1}{B_2}\right)} + B_3$	(7)
Temperature polarization in feed side (DCMD)	$T_{m,f} = \frac{h_m\left(T_p+\frac{h_f}{h_p}T_f\right)+h_fT_f-J_i\rho\Delta H_v}{h_m+h_f\left(1+\frac{h_m}{h_p}\right)}$	(8)
Temperature polarization in permeate side (DCMD)	$T_{m,p} = \frac{h_m\left(T_p+\frac{h_p}{h_f}T_p\right)+h_pT_p+J_i\rho\Delta H_v}{h_m+h_p\left(1+\frac{h_m}{h_f}\right)}$	(9)
Temperature polarization in feed side (VMD)	$T_{m,f} = T_f - \frac{J_i\rho\Delta H_v}{h_f}$	(10)

Table 2
Characteristics of the MD membranes used in this study (from the manufacturer)

Membrane materials	Pore size (μm)	Effective area (cm^2)	Membrane type	Wettability	Contact angle (°)	Porosity (%)
PVDF	0.22 0.45	12.2	Flat-sheet	Hydrophobic	145	75
PTFE	0.22 1.0	12.2	Flat-sheet	Hydrophobic	120.4	70

membrane. In VMD configuration (Fig. 2(b)), a vacuum pump was used to create a vacuum in the permeate membrane side. The range of vacuum was between 100 and 200 mbar. The vapor passing through the membrane was condensed in the cold trap and collected in the permeate tank, where an electronic balance was connected to measure the flux. In both systems, temperatures in feed sides and permeate sides were controlled using a water bath. Moreover, the recirculation flow rates ranged from 0.2 to 1.6 L/min.

Experiments were carried out under various operating conditions, The effects of membranes, feed temperature, degree of vacuum, flow rate, and feed solution on permeate flux were investigated for VMD membranes. Experiments under similar conditions were performed for DCMD membranes to compare

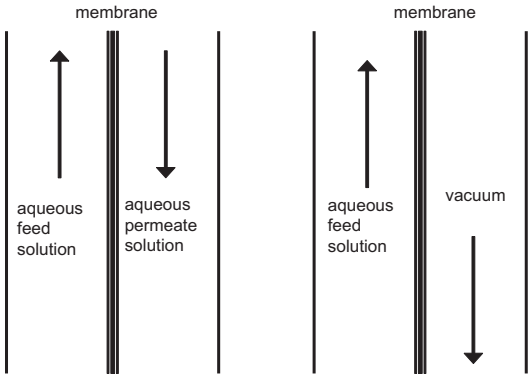

Fig. 1. Basic configuration for (a) DCMD and (b) VMD.

these two membrane systems. For DCMD, however, the effect of temperature difference on flux was examined instead of the effect of the degree of vacuum. Detailed operating conditions are summarized in Table 3.

4. Results and discussion

4.1. Direct Contact Membrane Distillation

First of all, a set of fundamental tests were performed in the DCMD system under various conditions. Then, the results were quantitatively compared with those in VMD system.

4.1.1. Effect of feed temperature

Fig. 3 shows the dependence of flux through MD membrane on time at various feed temperatures in the DCMD system. The PVDF membrane with the pore size of 0.22 μm was used for these tests. The permeate temperature was constant at 20˚C. The flow rates for feed and permeate were 24 and 15.6 L/h, respectively. As expected, the MD permeate flux increases with increasing the feed temperature due to an increased vapor pressure difference. At 50˚C of temperature difference between feed and permeate, the average flux was about 20 kg/m^2-h, which is almost five times than the flux at 20˚C of the temperature difference.

4.1.2. Effect of flow rate

Fig. 4 shows MD permeate flux at two different flow rate conditions in the DCMD system. The feed and permeate temperatures were 60 and 20 ˚C, respectively. It is evident from the plot that the high flow rate led to increased flux. This is attributed to the reduction in TP by increasing crossflow velocities at both membrane sides. Nevertheless, it is likely that the effect of flow rate on flux was less significant than that of feed temperature. With increasing the flow rate by 1.5 times, the permeate flux increase only by 1.25 times (12 kg/m^2-h → 15 kg/m^2-h).

4.1.3. Effect of feed salt concentration

Since MD uses vapor pressure difference, it is relatively less sensitive to the osmotic pressure of feed solution than RO. Thus, MD permeate flux is not highly dependent on salt concentration in feed solution. As shown in Fig. 5, less than 15% of flux reduction was observed in DCMD tests with an increase in feed concentration by five times.

4.2. Vacuum Membrane Distillation

4.2.1. Effect of feed temperature

Experiments were carried out using the VMD system under similar conditions to the DCMD case, as illustrated in Fig. 6. In VMD, the permeate temperature cannot be directly controlled. Instead, the degree of vacuum was controlled using a vacuum pump, which was set to 100 mbar for this test set. Same membrane (PVDF, 0.22 μm) was used under similar feed temperature conditions. Unlike the case of DCMD, permeate flux at low temperature was negligible. At 50˚C, the flux in DCMD was approximately 8 kg/m^2-h, while that in VMD was less than 1 kg/m^2-h. As increasing in the temperature, however, the flux in VMD rapidly increases. At 70 ˚C, the flux in DCMD was approximately 20 kg/m^2-h, while that in VMD was over 35 kg/m^2-h. (1) This is because of negligible heat transfer though the gas phase and membrane materials under reduced pressure conditions [12]. Based on these results, it is clear that the VMD has advantages over DCMD at high feed temperature conditions. Fig. 7 compares the average flux values for DMCD and VMD at different temperatures.

4.2.2. Effect of feed flow rate

Fig. 8 shows MD permeate flux at two different feed flow rate conditions in the VMD system. The feed temperature and degree of vacuum were 60˚C and 100 mbar, respectively. Just like DCMD, the flux in VMD also increases with increasing feed flow rate. The following equation was obtained from the linear regression of the experimental data:

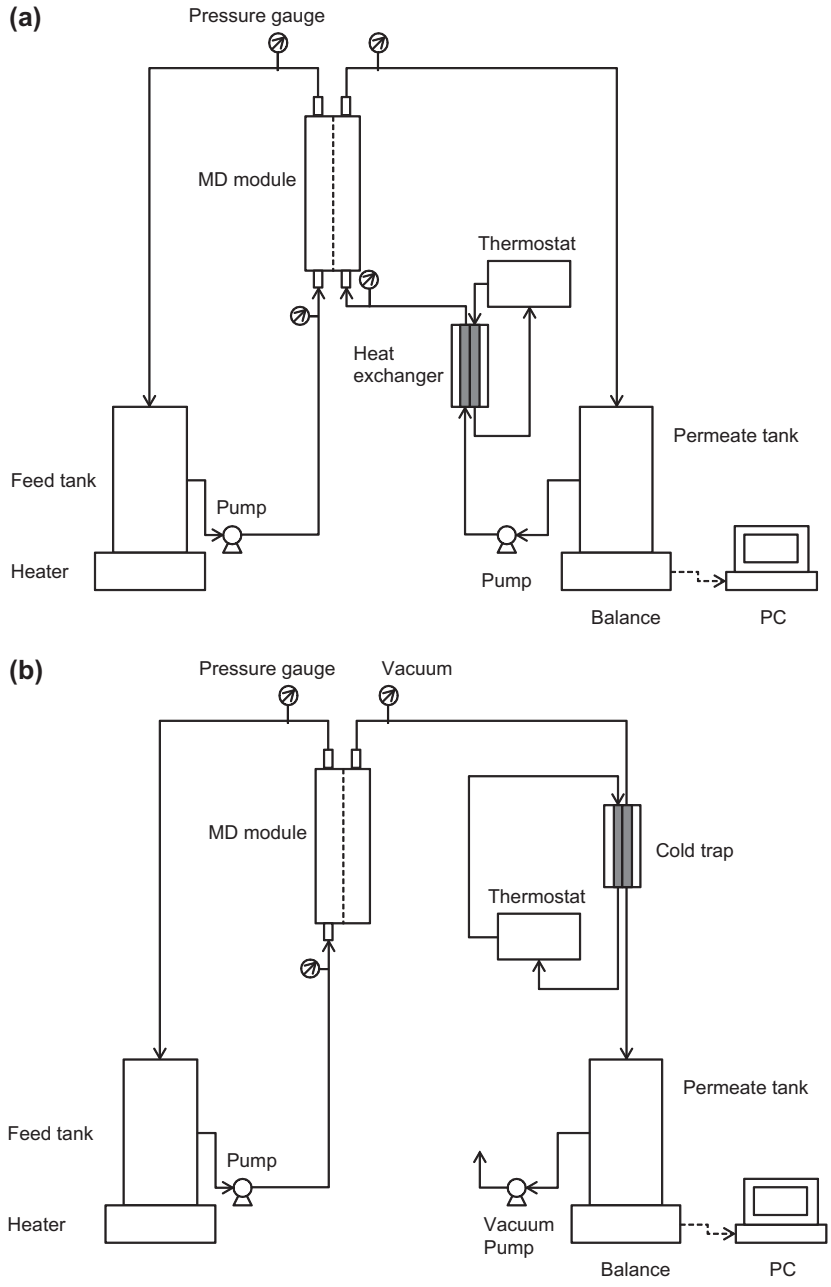

Fig. 2. Schematic diagram (a) DCMD system (b) VMD system.

$$J = 0.200Q + 7.61 \quad R^2 = 0.99 \text{ for DCMD} \tag{1}$$

$$J = 0.216Q + 5.68 \quad R^2 = 0.99 \text{ for VMD} \tag{2}$$

where J is the flux (kg/m^2-h) and Q is the flow rate (L/h). This suggests that the flux is almost linearly proportional to the flow rate at high flow rate conditions [2].

4.2.3. Effect of degree of vacuum

In VMD, the vacuum pressure in permeate side is related to the flux through the membrane because it affects the vapor pressure difference across the membrane. Fig. 8 shows the effect of the degree of vacuum on flux in the VMD system at two different flow rate (Q) conditions. The feed temperature was 60℃ for this test set. As expected, the flux increases

Table 3
Operating conditions of laboratory-scale MD systems

Item		Condition	
Operation type		DCMD	VMD
Effective membrane area		12.2 cm^2	12.2 cm^2
Flow rate	Feed	24, 36, 48 L/h	24, 36, 48 L/h
	Permeate	15.6, 24.0, 31.8 L/h	–
Membrane	PVDF	0.22, 0.45 μm	0.22, 0.45 μm
	PTFE	1.0 μm	1.0 μm
Solution	Feed	D.I water, 0.2, 0.5 1.0 M NaCl	D.I water, 0.2, 0.5 1.0 M NaCl
	Permeate	D.I water	–
Temperature	Feed	40, 50, 60, 70℃	40, 50, 60, 70℃
	Permeate	20℃	–
Vacuum pressure	Feed	–	–
	Permeate	–	100, 125, 150 mbar

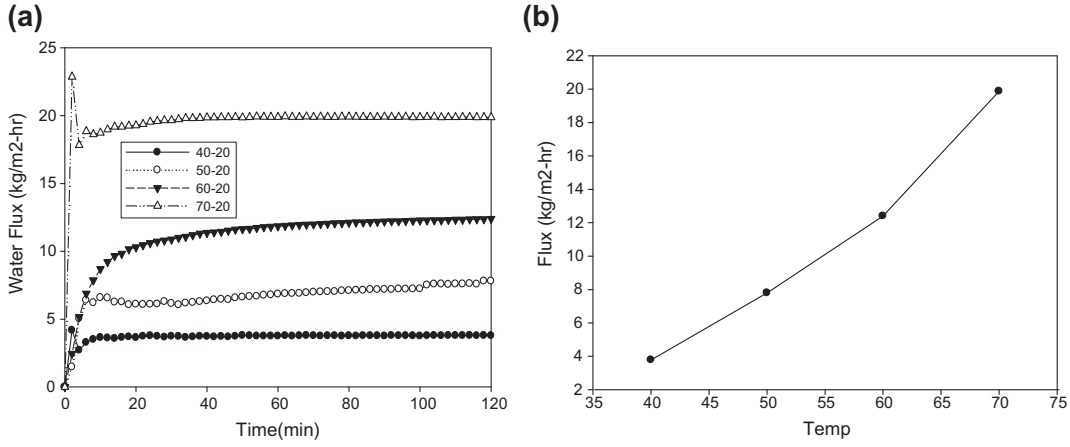

Fig. 3. Effect of feed temperature on flux in DCMD. (a) flux profiles (b) average flux. Experimental conditions: membrane – PVDF 0.22 μm; Q_{feed} = 24 L/h; $Q_{permeate}$ = 15.6 L/h; T_{feed} = 40, 50, 60, 70℃; $T_{permeate}$ = 20 ℃; feedwater—D.I. water.

with decreasing vacuum pressure [11]. Under higher flow rate conditions, the effect of the degree of vacuum becomes more important. A linear regression between the degree of vacuum and water flux indicated that the absolute values of the slope are 0.148 kg/m^2-h-mbar at Q = 24 L/h and 0.261 kg/m^2-h-mbar at Q = 48 L/h, respectively. This suggests that the flux is more sensitive to flow rate at higher flow rate conditions (see Fig. 9).

4.2.4. Effect of feed salt concentration

Fig. 10 shows the effect of NaCl concentration on flux in the VMD system. As also shown in DCMD system, the flux slightly decreases with increased feed concentration in VMD. This suggests that VMD as well as DCMD can be applied for seawater desalination of high recovery ratio [3].

4.2.5. Effect of membrane material and pore size

In the VMD system, flux profiles for different membranes were compared as shown in Fig. 11. The feed temperature was 60℃ and the degree of vacuum was 100 mbar. In case of PVDF membrane with the pore size of 0.45 μm, the flux was unstable from the beginning, indicating that the membrane wetting occurred. In case of PTFE membrane with the pore

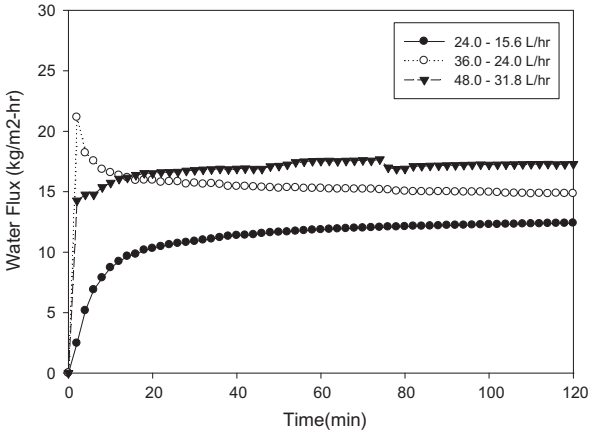

Fig. 4. Effect of feed and permeate flow rates on flux in DCMD. Experimental conditions: membrane – PVDF 0.22 μm; T_{feed} = 60˚C; $T_{permeate}$ = 20˚C; feedwater—D.I. water.

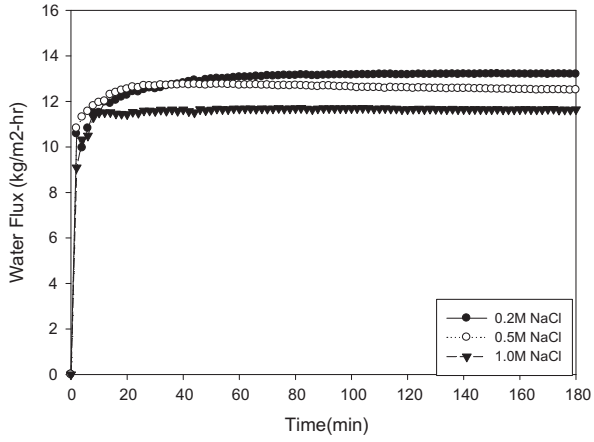

Fig. 5. Effect of NaCl concentration of feed solution on flux in DCMD. Experimental conditions: membrane – PVDF 0.22 μm; Q_{feed} = 24 L/h; $Q_{permeate}$ = 15.6 L/h; T_{feed} = 60˚C; $T_{permeate}$ = 20˚C, feedwater—0.2, 0.5, and 1.0 M of NaCl solutions.

size of 1.0 μm and PVDF membrane with the pore size of 0.22 μm, the membranes were not wetted. According to the manufacturer's specification, the bubble points for PVDF 0.22 μm, PVDF 0.45 μm, and PTFE 1.0 μm membranes were 1.24, 0.56, and 1.0 bar, respectively. Considering the pressure difference between the feed and permeate in the VMD, it appears that the PVDF 0.22 μm membrane is the most appropriate. Although PTFE 1.0 μm membrane showed a higher flux than PVDF 0.22 μm membrane, its bubble point (~1.0 bar) seems to be too close to the pressure difference (~0.9 bar).

4.3. Theoretical analysis

A simple model was applied to further investigate DCMD and VMD systems as described in Table 1. To begin, the model was verified and calibrated using the experimental results. All the parameters for the membrane materials were obtained in the literature. To estimate CP and TP, the Sherwood and Nusselt

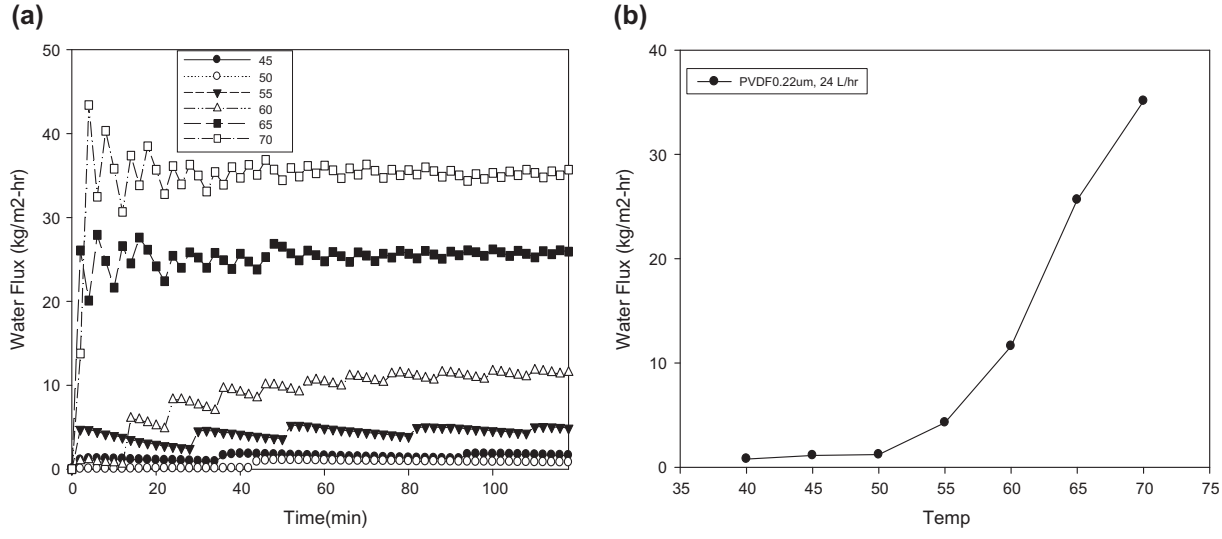

Fig. 6. Effect of feed temperature on flux in VMD. (a) flux profiles (b) average flux. Experimental conditions: membrane – PVDF 0.22 μm; Q_{feed} = 24 L/h; $Q_{permeate}$ = 15.6 L/h; T_{feed} = 45, 50, 55, 60, 65, 70˚C; P_{vacuum} = 100 mbar; feedwater—D.I. water.

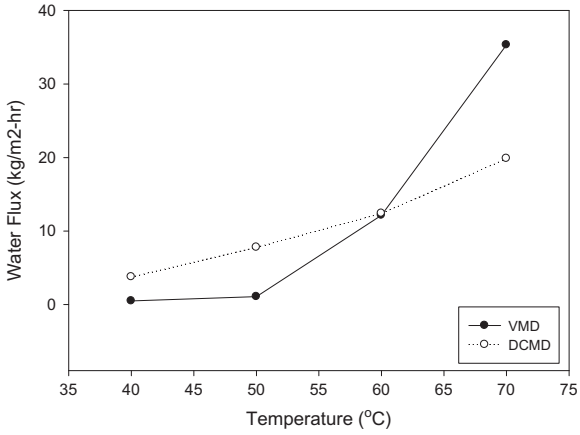

Fig. 7. Comparison of average flux for DCMD and VMD at different temperatures.

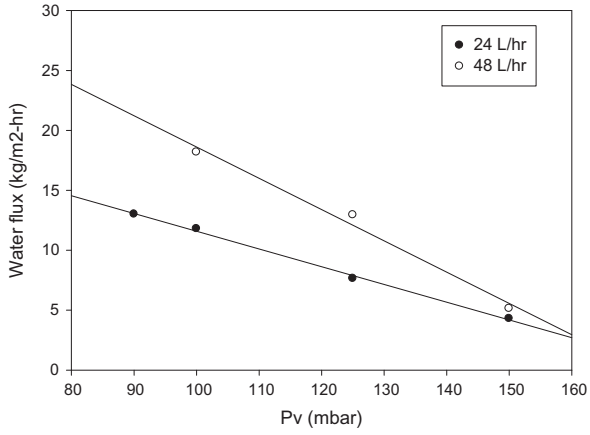

Fig. 9. Effect of degree of vacuum on flux in VMD. Experimental conditions: membrane–PVDF 0.22 μm; Q_{feed} = 24, 48 L/h; T_{feed} = 60°C; feedwater—D.I. water.

correlations were used. In addition, the parameters related to heat losses through the membrane were determined by non-linear regression with experimental data. Based on this approach, TP values were estimated to 0.59 for DCMD and 0.87 for VMD. Depending on the temperature, TP values were a little bit different but they were assumed to be constant in each configuration for simple calculation. As show in Fig. 12, the model fits the experimental data well.

Using the model, the efficiency of DCMD and VMD can be compared under various conditions. From previous results, it is clear that VMD showed higher flux at high feed temperature and high flow rate. Based on the model analysis, it is attributed to the degree of vacuum used in this study. According to the Antoine equation, the vapor pressure at 20°C is about 23 mbar while the lowest vacuum pressure in our tests was 90 mbar. Although other factors can affect the water vapor transport through the membrane, the degree of vacuum appears to be insufficient to show higher flux in VMD than DCMD. Nevertheless, the effect of vacuum and other factors become more important at high temperature or high flow rate conditions, allowing higher flux in VMD than DCMD.

Fig. 13 shows the simulation results using the model for seawater desalination under various recovery ratios. Here, the recovery is defined as the ratio of permeate (produce water) to the feedwater, which is also the water yield of operation. Again, the feed temperature was 60°C and the permeate temperature for DCMD and degree of vacuum for VMD were 20°C

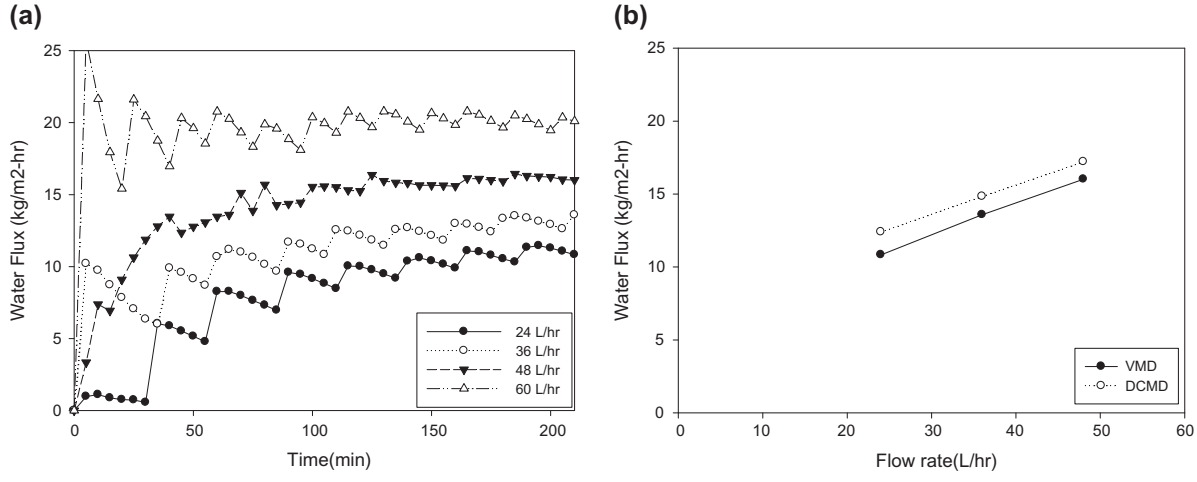

Fig. 8. Effect of feed flow rate (a) flux profiles, (b) comparison of VMD with DCMD. Experimental conditions: membrane–PVDF 0.22 μm); T_{feed} = 60°C; P_{vacuum} = 100 mbar; feedwater—D.I. water.

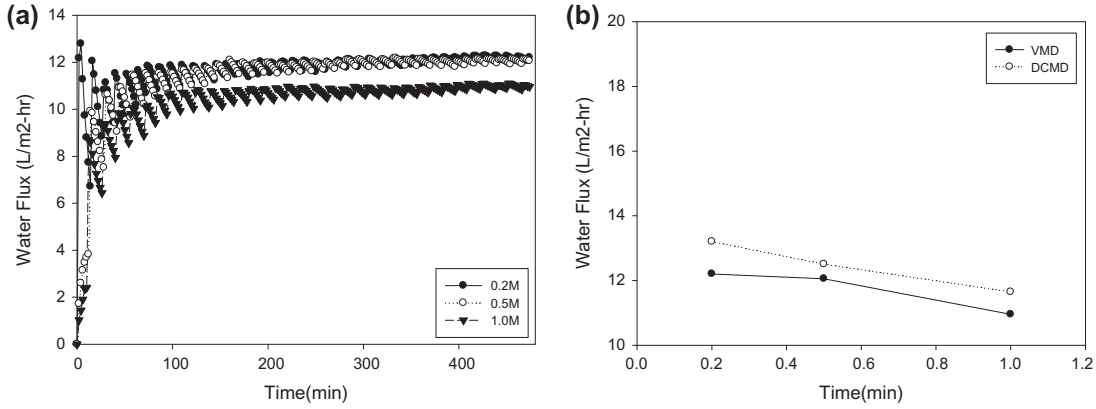

Fig. 10. Effect of NaCl concentration of feed solution on flux in VMD (a) flux profiles (b) comparison of VMD with DCMD. Experimental conditions: membrane–PVDF 0.22 μm; $Q_{feed} = 24$ L/h; $P_{vacuum} = 100$ mbar; $T_{feed} = 60$°C; feedwater—0.2, 0.5, and 1.0 M of NaCl solutions.

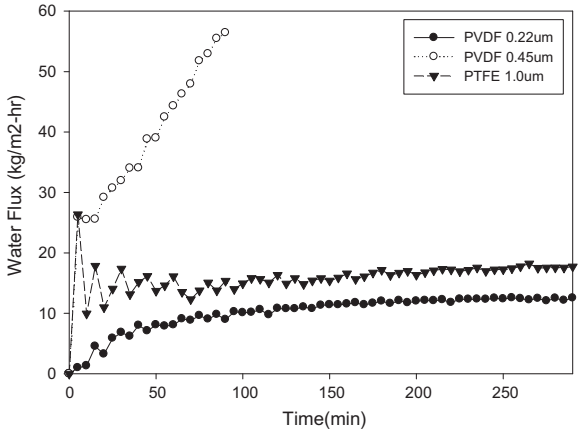

Fig. 11. Effect of membrane type on flux in VMD. Experimental conditions: membrane–PVDF 0.22 μm, PVDF 0.45 μm, and PTFE 1.0 μm; $Q_{feed} = 24$ L/h; $P_{vacuum} = 100$ mbar; $T_{feed} = 60$°C; feedwater–D.I. water.

and 100 mbar, respectively. Initially, two MD systems result in similar performances. Nevertheless, the permeate flux decreases with increasing recovery up to 0.6, which corresponds to the salt concentration over 1.5 M. At higher recovery, the flux in DCMD was higher than that in VMD due to relatively high vacuum pressure (= 100 mbar). Although the data are not shown, the flux in VMD may be higher than that in DCMD under lower vacuum pressure conditions (or higher degree of vacuum).

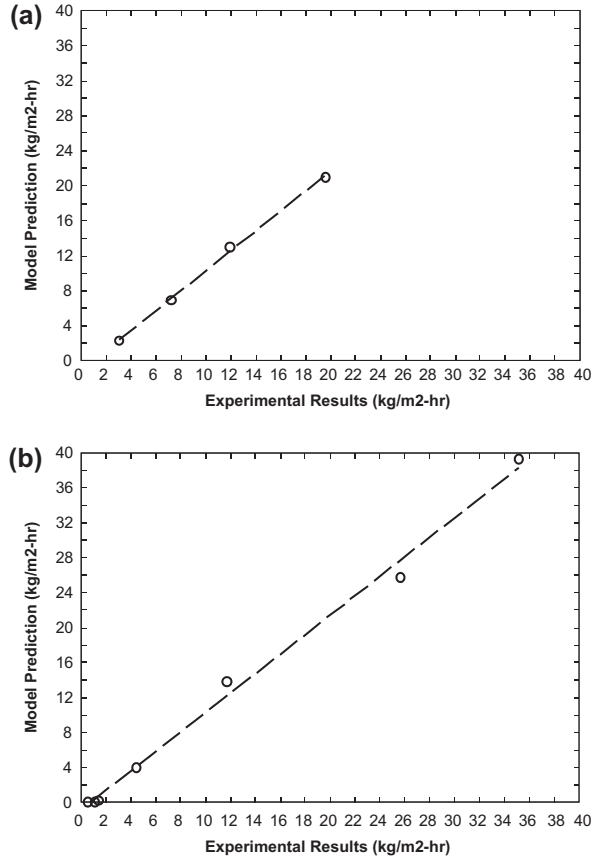

Fig. 12. Comparison of model calculation with experimental data (a) DCMD and (b) VMD.

5. Conclusions

In this work, the flux of DCMD and VMD was compared under various conditions to provide insight into the design and optimization of MD systems. The following conclusions can be drawn:

(1) At low feed temperature, the flux in the DCMD system was higher than that in the VMD system. Based on the theoretical analysis, it is likely that the relatively low degree of vacuum (>90 mbar) is the main reason for this trend.

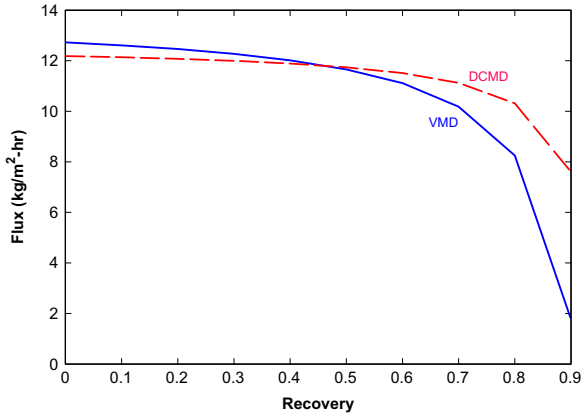

Fig. 13. Simulation of seawater desalination process using the MD model. Model conditions: membrane–PVDF 0.22 μm; Q_{feed} = 24 L/h; $Q_{permeate}$ = 15.6 L/h; P_{vacuum} (VMD) = 100 mbar; T_{feed} = 60 ℃; feedwater—0.6 M of NaCl solutions (synthetic seawater).

(2) At high feed temperature, the flux in the VMD system became higher. This is because of negligible heat transfer though the gas phase and membrane materials under reduced pressure conditions.
(3) The effect of flow rate was more important in the VMD system than in the DCMD system. The flux in the VMD system was almost linearly proportional to the flow rate within the test conditions in this study.
(4) PVDF membrane with an average pore size of 0.45 μm was not suitable for the VMD operation due to its low entry pressure. Since it could be used in the DCMD systems, it appears that the optimum membrane for DCMD and VMD should be different.
(5) A simple model was applied to analyze and predict the performance of MD systems, allowing better understanding of the characteristics of different MD configurations

Nomenclature

B_i	—	transport coefficient in MD (kg/m^{2}s Pa)
B_1	—	transport coefficient for Knudson diffusion (kg/m^{2}s Pa)
B_2	—	transport coefficient for molecular diffusion (kg/m^{2}s Pa)
B_3	—	transport coefficient for Poiseuille flow (kg/m^{2}s Pa)
C_s	—	salt concentration (M)
ΔH_v	—	heat of vaporization (kJ/kg)
h_f	—	heat transfer coefficient in the feed boundary layer (W/m^2-K)
h_m	—	heat transfer coefficient in the membrane (W/m^2-K)
h_p	—	heat transfer coefficient in the permeate boundary layer (W/m^2-K)
J_i	—	permeate flux
M	—	molecular weight of water (kg/mol)
P_m	—	average partial pressure in the membrane pore (Pa)
p_w	—	vapor pressure of aqueous solution (Pa)
p_w^0	—	vapor pressure of pure water (Pa)
R	—	gas constant (J/mole-K)
r	—	pore radius of membrane (m)
T	—	temperature (K)
T_m	—	average temperature of the membrane (K)
$T_{m,f}$	—	temperature at the feed membrane surface (K)
$T_{m,p}$	—	temperature at the permeate membrane surface (K)
T_f	—	feedwater temperature (K)
T_p	—	permeate temperature (K)
γ_{ln}	—	reciprocal of the drafting factor
δ	—	thickness of the membrane (m)
μ	—	viscosity of the vapor (Pa-s)
ε	—	porosity of the membrane
ρ	—	density of water (kg/m^3)
τ	—	tortuosity of the membrane

Acknowledgments

This research was supported by a grant funded by Kookmin University and the National Research Foundation of Korea Grant funded by the Korean Government (MEST) (NRF-2010-0029061).

References

[1] K.W. Lawson, D.R. Lloyd, Membrane distillation, J. Membr. Sci. 124 (1997) 1–25.
[2] A. Alkhudhiri, N. Darwish, N. Hilal, Membrane distillation: A comprehensive review, Desalination 287 (2012) 2–18.
[3] T. Mohammadi, M. Akbarabadi, Application of PVDF membranes in desalination and comparison of the VMD and DCMD processes, Desalination 181 (2012) 25–41.
[4] S. Cerneaux, I. Strużyńska, W.M. Kujawski, M. Persin, A. Larbot, Comparison of various membrane distillation methods for desalination using hydrophobic ceramic membranes, J. Membr. Sci. 337 (2009) 55–60.
[5] M. Mulder, Basic principle of membrane technology, 2nd ed., Springer, Berlin, 1996.
[6] L. Martinez, F.J. Florido-Diaz, A. Hernandez, P. Pradanos, Characterization of three hydrophobic porous membranes used in membrane distillation. Modelling and evaluation of their water vapour permeability, J. Membr. Sci. 203 (2002) 15.

[7] V.V. Ugrozov, I.B. Elkina, V.N. Nikulin, L.I. Kataeva, Theoretical and experimental research of liquid-gap membrane distillation process in membrane module, Desalination 157 (2003) 325.
[8] A.S. Jonsson, R. Wimmerstedt, A.C. Harrysson, Membrane distillation, a theoretical study of evaporation through microporous membranes, Desalination 56 (1985) 237.
[9] M.S. El-Bourawi, Z. Ding, R. Ma, M. Khayet, A framework for better understanding membrane distillation separation process, J. Membr. Sci. 285 (2006) 4.
[10] H. EI-Dessouky, H.I. Shaban, H. AI-Ramadan, Steady-state analysis of multi-stage flash desalination process, Desalination 103 (1995) 271–287.
[11] T. Mohammadi, M.A. Safavi, Application of Taguchi method in optimization of desalination by vacuum membrane distillation, Desalination 249 (2009) 83–89.
[12] H. Fan, Y. Peng, Application of PVDF membranes in desalination and comparison of the VMD and DCMD processes, Chem. Eng. Sci. 79 (2012) 94–102.